J. Condensed Matter Nucl. Sci. 9 (2012) 21–29

Research Article

Evidence for the Induction of Nuclear Activity in Polarized Pd/H–H_2O System

Stanislaw Szpak *
SPAWAR Systems Center San Diego, San Diego, CA 92152, USA

Jack Dea†
4809 Clairemont Drive, San Diego, CA 92117, USA

Abstract

In cells employing cathodes prepared by the co-deposition process, the polarized Pd/D–D_2O system becomes nuclear active when the concentration of deuterium, expressed as D/Pd atomic ratio, is equal to or greater than one. In contrast, to activate the polarized Pd/H–H_2O system, action of an external magnetic field, modulation of cell current or both, are required. Evidence for the nuclear active state in the Pd/H–H_2O system namely deuterium production, particle emission and catastrophic thermal event, is presented.
 ISSN 2227-3123

Keywords: Co-deposition, Coupled reaction, Magnetic field, Pd/H–H_2O system

1. Introduction

Recently Widom and Larsen [1] presented a novel approach to explain the induction of a nuclear active state in the polarized Pd/D–D_2O system. In their approach, an electron capture by the deuteron is responsible for the system's behavior. Their model implies that, under the same conditions, the energetically less demanding Pd/H–H_2O system should show signs of nuclear activity, but this has not been reported. To resolve this issue, we reviewed [a] the available empirical evidence and concluded that the proper course of action is to examine in detail the content and meaning of the reaction

$$e^- + p^+ \rightarrow n + \nu. \quad (1)$$

Nuclear reactions of this type can be treated as chemical reactions [2,3]. Consequently it is not difficult to write down the thermodynamic conditions for the reaction to proceed, namely the inequality $\mu(e^-) > \mu(n) - \mu(p^+) > 0$.

*Retired. Present address: 3498 Conrad Ave., San Diego, CA 92117, USA.
†E-mail: eepsd@yahoo.com
[a]Division of labor: JD – data collection, SS – data interpretation.

 ISSN 2227-3123

Since the neutrinos are not retained by matter, the chemical potential of the neutrinos will not appear in the equation of equilibrium or reaction kinetics. Equation (1) provides only limited information, namely it is the statement of conservation of mass, energy and charge. Since the initial and final states are not specified, it simply means that the system consists of unbounded particles in the sense that there is a continuous range of possible energies. All protons located in the reaction volume interact with the Pd lattice to a various degree. The chemical potential of interacting protons p_I^+ is of the form $\mu(p_I^+) = \mu(p^+) + u(r)$, where $u(r)$ denotes the energy of interaction. To evaluate the $u(r)$ function, we consider the relation $\mu(p) = \varepsilon(-p)$, i.e. the chemical potential of a particle p is its negative binding energy In this representation the $u(r)$ function indicates that a part of the interacting site is incorporated into the proton itself, i.e. it represents the degree of an overlap which, in turn, determines whether or not the electron capture by proton can occur. For an electron capture by a proton to occur, the quantity $\mu(n) \ -\mu(p_I^+)$ must be positive Since light water electrolysis does not produce a nuclear active state, it follows that $\mu(p_I^+)$, is greater than that of the neutron, $\mu(n)$, i.e. irrespective of its energy the electron capture reaction cannot occur. In Section 2 of this communication, we describe the procedure that reduces the interaction energy of the palladium/lattice defect, in Section 3 we present evidence for nuclear activity in Section 4 we offer interpretation of a few selected cases using methods and terminology commonly employed in chemical research.

2. Effect of an External Magnetic Field

The interaction of a magnetic field with electrochemical systems can be divided into three main areas: (i) magneto-hydrodynamic effects, i.e. those affecting mass transport via the reduction of the diffusion layer thickness, (ii) magneto-mechanical effects, i.e. those that involve the shape change of micro-globules as well as complex macro-molecules, and (iii) non-specific interactions of electronic nature, i.e. those affecting dynamics of the highly concentrated hydrogen in the Pd lattice. These effects are attributed to forces generated by the gradients of magnetic energy density, i.e. by forces that arise from non-homogeneity of the paramagnetic entity and those associated with non-uniformity of the magnetic field. Of interest to the present communication is the effect on the structure of the deposit, the magneto-mechanical effect, and on the process(es), the non-specific interactions.

2.1. Magneto-mechanical effects

The effect of an external magnetic field, (ca 0.2 T) on a single globule and on the deposit, including the interphase, is briefly discussed.

2.1.1. *Single micro-globule*

In the absence of an external magnetic field, the SEM photograph shows that the Pd/H deposit has a "cauliflower" structure consisting of almost spherical micro-globules, Fig. 1a. When placed in an external magnetic field, its structure changes. The almost spherical micro-globules are flattened to form a "star-like" appearance, Fig. 1b.

2.1.2. *The Pd/H deposit and the interphase*

As a general information, we note that when the Pd/H deposit is placed in an external magnetic field the magnetic "order" of one layer (interphase) affects the "order" of another layer (bulk) being in contact with the first. The change in the deposit morphology affects the distribution of absorbed hydrogen. Any motion of hydrogen within the interphase generates stresses that, in turn, produce dislocation and other types of interaction sites. That it is to say within the interphase exists a state of dynamic equilibrium which governs the distribution of hydrogen interacting with

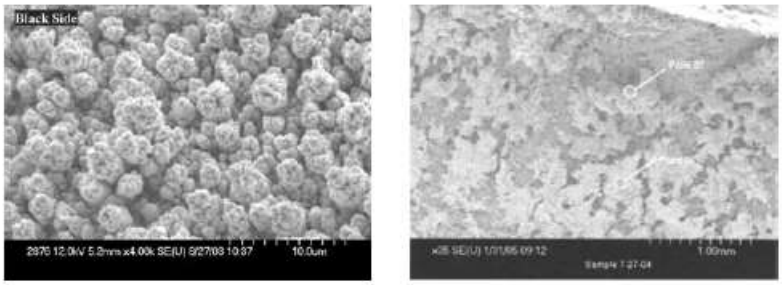

Figure 1. (a) SEM photo of electrode surface with no magnetic field applied. (b) Electrode surface with applied magnetic field.

the palladium lattice which means that some interaction sites are formed, other disappear thus releasing the interacting protons and making them available for the electron capture reaction.

2.2. Non-specific interactions

In general: When the "host/guest" complexes (where the Pd lattice defect acts as the host for the guest $p_l^+ e^-$ complexes) are exposed to magnetic field, deformation of their structure is very likely to occur due to magnetic torque. Here, we address the effect of magnetic field on strength of Pd/lattice defect interaction and rate of transport.

2.2.1. *Sequence of events and strength of interaction*

The sequence of events leading to the initiation of the nuclear active state is shown in Fig. 2. Here, the events within the metal side of the interphase are: an exchange between the adsorbed and absorbed hydrogen, H_{ad} H_{ab} the transition from atomic to nuclear state denoted $H_{ab} \rightarrow p^+$, followed by $p^+ \rightarrow p_l^+$, the latter identifies a proton interacting strongly with

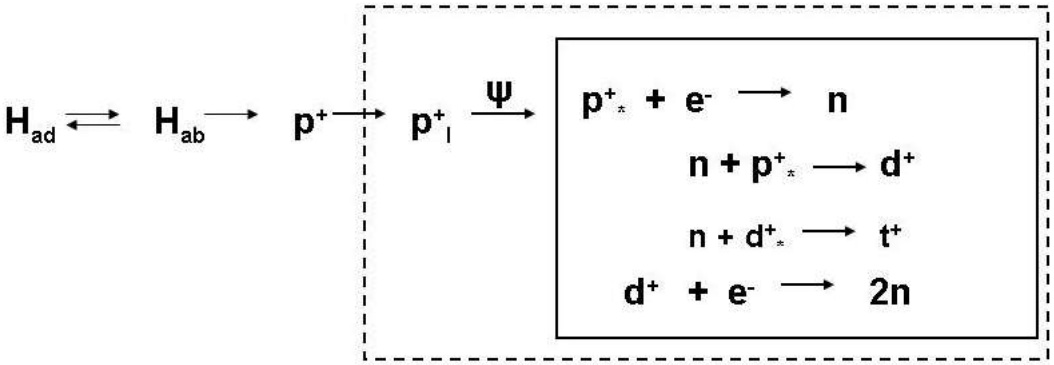

Figure 2. Schematic diagram showing events within the interphase. Enclosed by *broken line* are processes affected by an external field; by *solid line* coupled nuclear reactions.

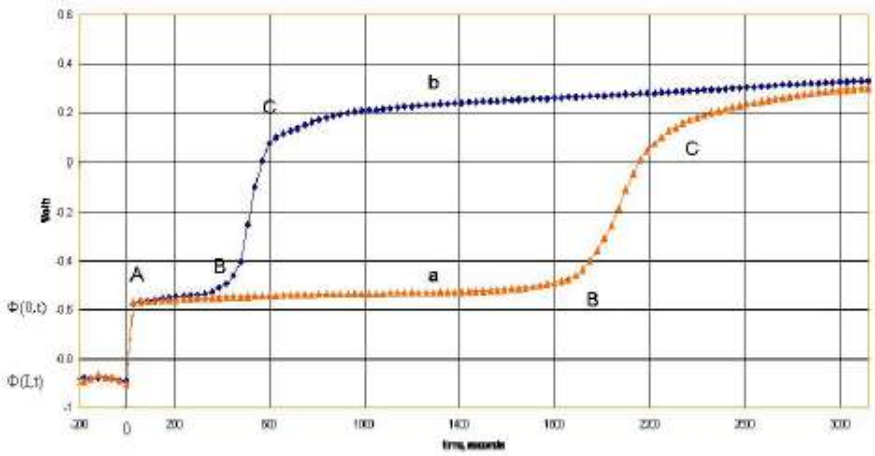

Figure 3. Hydrogen desorption rates. *Curve a* in the absence of magnetic field. *Curve b* in the presence of external field.

the Pd lattice. When an external magnetic field, ψ is applied, a new set of processes can be identified, viz weakening of the interaction, $p_l^+ \rightarrow p_*^+$ electron capture by proton $e^- + p_*^+ \rightarrow n$, with neutrons either escaping or reacting with proton to yield deuteron, $n + p_*^+ \rightarrow d^+$ and an electron capture by deuteron yielding two neutrons $e^- + d^+ \rightarrow 2n$.

2.2.2. *Rate of transport (desorption)*

The data presented in Fig. 3 show a typical potential/time curve for the desorption of hydrogen from the electrode having structure shown in Fig. 1b, in the absence and presence of an external magnetic field, curves a and b, respectively. Here, the electrode potential/time relation, $\Phi(t)$, shows that the time for the transition from transport to surface controlled desorption of hydrogen, segments AB and BC, is substantially shorter when an external magnetic field was applied. Such behavior indicates that magnetic field weakens the proton/Pd defect interaction, i.e. $\mu(p_l^+) > \mu(p_*^+)$.

3. Evidence of Nuclear Activity

In what follows, we present description of experimental protocol, evidence of nuclear activity based on deuterium production, neutron emission and catastrophic thermal behavior.

3.1. Experimental protocol

A rectangular vessel, made of clear plastic, served as the electrochemical cell, Fig. 4. The cathode assembly is shown in Fig. 4a. A stock of two CR-39 chips is attached to a plastic strip and one placed outside the cell. A platinum wire, in the indicated shape, served as a substrate for the co-deposited Pd/H film. The assembled cathode is inserted into the cell. The fabrication of cathodes involves co-deposition. The co-deposition is a process whereby the palladium is deposited in the presence of evolving hydrogen from a Pd^{2+} salt solution onto a substrate that does not absorb hydrogen. The structure of the electro-deposited palladium is controlled by the solution composition and the cell current profile. To assure acceptable deposits, one starts at current density less than its diffusion controlled value. Here, for the co-deposition from a solution of 0.03 M $PdCl_2$ and 0.3 M LiCl dissolved in H_2O, the current profile was as follows:

$i = -1.0$ mA cm^{-2} for the first 24 h followed by $i = -3.0$ mA for the time required to reduce all the Pd^{2+} ions; (b) a 3–4 h stabilization period at $i = 30$ mA. When the co-deposition is completed the cell is placed in an external magnetic field as shown in Fig. 3. Upon placing an operating cell in a magnetic field the electrochemical compression of absorbed hydrogen was put under computer controlled regime with $i = -400$ mA for 90 s and $i = 5.0$ mA for 5 s.

3.2. Deuterium detection

The mass spectrograph was used to analyze for deuterium. The Pd/H film co-deposited onto a thin coiled palladium wire was employed to assure retention of the electrochemically compressed hydrogen isotopes (Fig. 4b). This electrode design was selected to meet the requirements imposed by mass spectrograph. To minimize the desorption of hydrogen isotopes the following procedure was adapted (a) remove the cell from magneto-static field, (b) stop the cell current flow, (c) take out the cathode, (d) cut-off the coiled part of the cathode, (e) place the sample in mass spectrograph, (f) evacuate to ca 10^{-5} torr, (g) turn on mass spectrograph, (h) set the atomic number of interest, and (i) print results. The mass spectroscopic analysis, performed upon completion of a run, showed the presence of all hydrogen isotopes. Qualitatively, deuterium was the dominant isotope with negligible amounts of tritium. Typically, the D/H atomic ratio greater than one, with a value as high as 5.1, was recorded. Needless to say that the presence of deuterium in the cathode is of utmost importance because it might provide decisive insight into the mechanism of nuclear reactions in condensed matter. As a rule, mass spectroscopic analysis yields results that are unambiguous. However if additional verification is required, then this can be done by measuring the D/H atomic ratios following electrolysis of water with known concentration of D_2O [4], a method used by us.

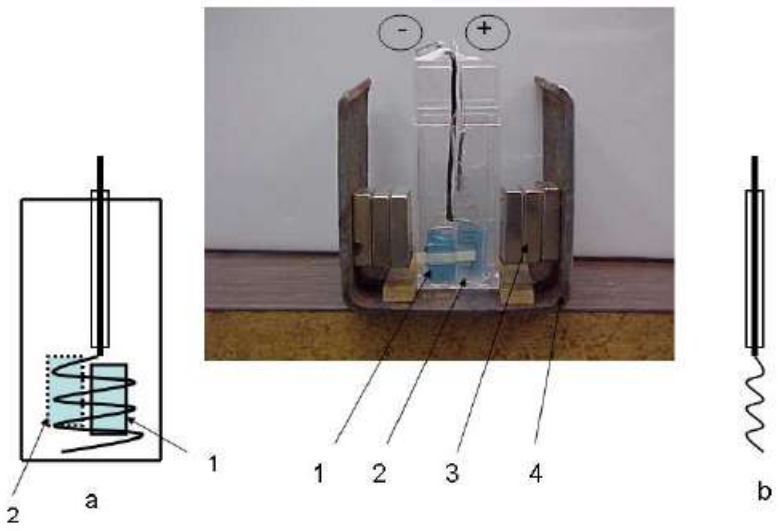

Figure 4. Electrochemical cell. (1) Outside CR-39 detector, (2) double CR-39 stock located inside cell, (3) neodymium magnets, (4) magnet holder Cathode assembly designed for, (a) neutron detection, 1–CR-39 chips inside the cell, 2–CR-39 outside the cell; (b) for determination of deuterium content.

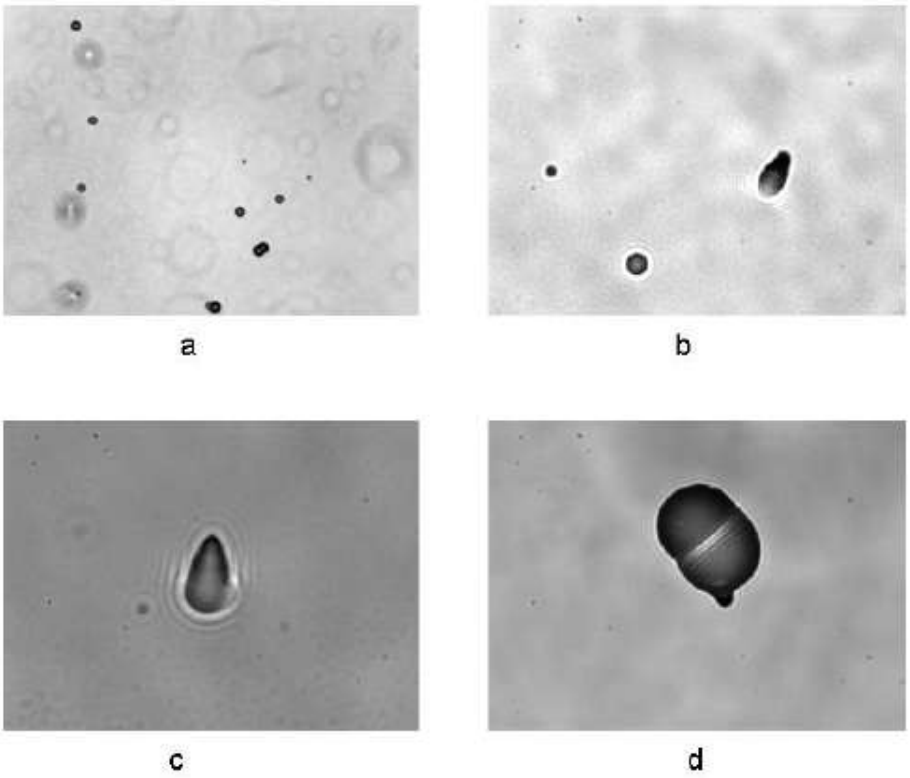

Figure 5. Images of tracks in CR-39 detectors created in the course of an experiment: (a) distribution of tracks at 40×, (b) illustrates the angle of impingement at 500×, (c) shows a single track at 1000×, and (d) image of a double track at 500×.

3.3. Neutron detection

Figure 5 shows typical images of tracks recorded on CR-39 chips. The examination of the CR-39 chips, located inside and outside, indicates no difference in the type of tracks but in their number, the latter being highest on the CR-39 detector facing the cathode and the lowest on the chip located outside the cell. In particular, Fig. 5a shows a typical distribution of images of circular and elliptical tracks, Fig. 5b and 5c illustrate the case of ionizing particle entering either perpendicular to the detector's surface or at an oblique angle, and Fig. 5d a double track. The physical meaning of the images recorded by CR-39 detectors is discussed in detail by Mosier-Boss et al. [5].

3.4. Catastrophic thermal events

Several catastrophic thermal events were observed (three out of ten). In one case, after three days of electrolysis with cell current varying between -300 and 5 $\mathrm{mA\,cm^{-2}}$, a catastrophic thermal event has occurred that resulted in cell deformation, loss of electrolyte due to evaporation and leaking through a punctured cell bottom (Fig. 6). The damage, about 1/3 of total area, viewed from the outside, Fig. 6a, and inside the cell, Fig. 6b, is consistent with placing a very hot object in contact with plastic material. The intensity of the heat source can be estimated from the temperature raise of the electrolyte during the last 170 min of cell operation Fig. 7. In a another run, a cell, charged with 3.0 ml of 0.03 M

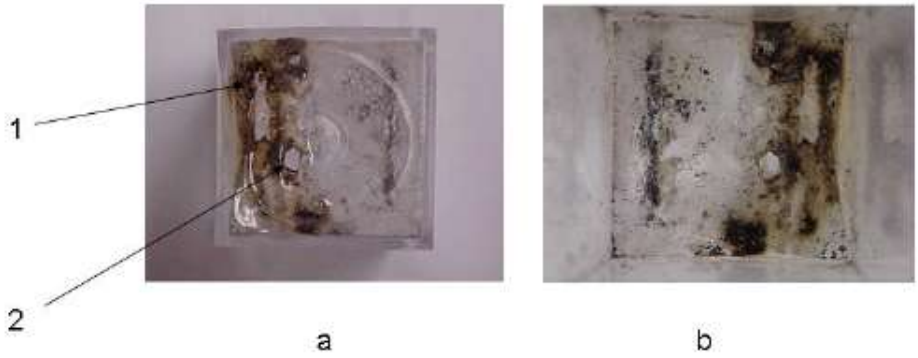

Figure 6. Damaged cell bottom: (a) outside view, (b) inside view. *Arrows* indicate the well-defined damage areas (1–embedded particles, 2–hole).

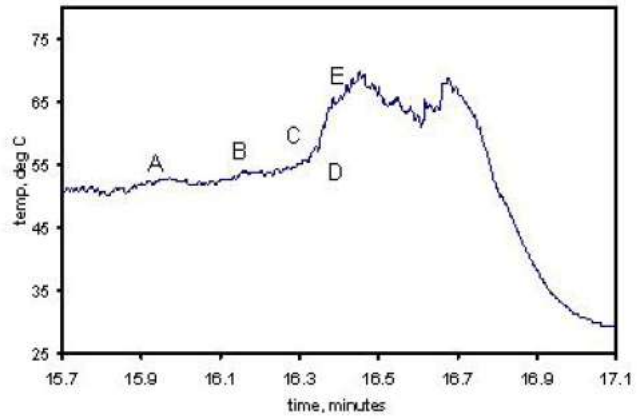

Figure 7. Temperature profile during thermal run-away

$PdCl_2$ and maintained at a constant volume of 5.0 ml, was operated for two days before recording the temperature with the thermocouple located below the cathode. Within the last 160 min the electrolyte temperature remained constant (at 50°C) followed by, at first, a slow raise for the next four minutes, section ABC, followed by a rapid increase at 2.6°C/s, section DE. During the next 3–4 min, the electrolyte evaporated and the temperature returned to ambient. For this run, the intensity of the heat source, based on the heat generated by the minute amount of the PD/H film and transferred to the electrolyte, can be estimated to be more than 10 eV/Pd atom, i.e. outside the limits of chemical reaction. Furthermore the temperature raise of the source of ca 250°C/s. means that substantial amount of the electrolyte was lost by "film boiling".

3.5. Mechanism of the Pd/H film separation

A probable, but speculative, mechanism of Pd/H film separation from the Pt substrate can be deduced using photograph, Figs. 8a and 8b. The separation shown in Fig. 8 illustrates the separation of a Pd/D deposit in another set of experiments.

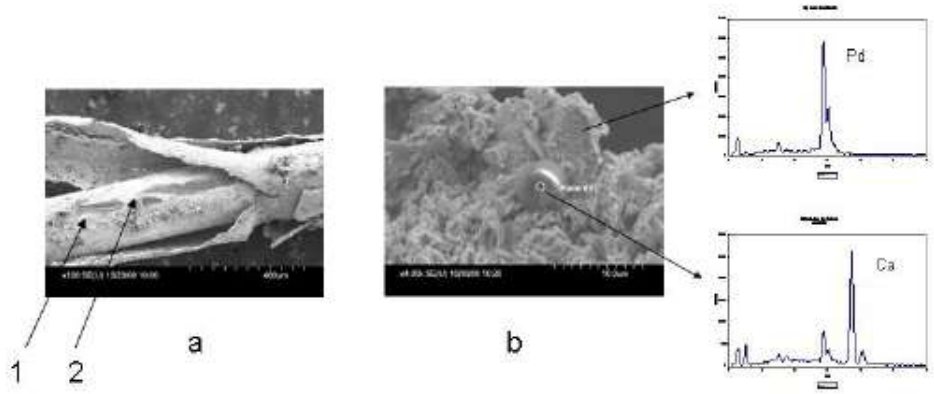

Figure 8. (a) SEM/EDX SEM photograph illustrating separation of a Pd/H film during a mild run-a-way run. (b) SEM photograph showing single reaction site; *top chart*–EDX of Pt substrate; *bottom chart*–EDX showing localized transmutation.

In particular examination of Fig. 8a suggests the following: (i) a number of localized reactions at the Pt/Pd/D interface, indicated by an arrow, forced the separation of the Pd/D deposit from the Pt substrate (ii) the SEM/EDX analysis of reaction sites contains participation of a nuclear event (transmutation) is involved in forcing film separation. The Pd/H film separation shown in Fig. 8 occurred during a mild thermal run-away during electrolysis of light water is almost identical to that heavy water, thus suggesting the same mode of separation.

The film separation may be explosive. The damage, shown in Figs. 8a and 8b, indicates that a Pd/H sleeve after separation was propelled away from the cathode and came in contact with the cell bottom. The high temperature and the amount of thermal energy necessary to generate the observed damage implies that thermal activity did not terminate upon separation from the cathode but persisted during flight as well as after landing at the cell bottom.

4. Closing Remarks

We prepared this communication to disclose that it is possible to extend the Fleischmann–Pons effect to the Pd/H–H_2O system. This extension is reproducible provided that the described procedure is followed and, in particular, that the Pd/H co-deposition is done carefully Because of its introductory nature, some interpretations of experimental evidence are certain other are speculative.

4.1. Cases of certain interpretation

There are two cases where the interpretation appears to be certain, namely: (i) the $e^- + p^+ \rightarrow n$ reaction starts the induction of the nuclear active state in the Pd/H–H_2O system and (ii) the transition $p_l^+ \rightarrow p_*^+$ is the low-energy process that generates the condition for the reaction $e^- + p_*^+ \rightarrow n$ to occur.

4.2. Case of speculative interpretation

One of the unresolved problems, associated with the Fleischmann–Pons effect, is the origin of the catastrophic thermal run-a-way There is little factual information on which to arrive at a probable model. In an attempt to get some understanding, from the many reported cases, we selected two involving the Pd/D–D_2O and one a mixed

Pd/D//Pd/H –H_2O systems. The first, at the University of Utah in Prof. Pons laboratory [6], the second described by Biberian [7] and the third reported in this communication. The available factual information: In the first case – cathode size (volume) 1.0 cm^3 explosion occurred at night; damage: cell destroyed, a hole in the laboratory bench, light damage to laboratory floor. On the second case – cathode volume 0.11 cm^3; damage experimental set-up destroyed. In the third case – cathode volume 0.01 cm^3; minor damage (cf. Fig. 6). It appears that the severity of damage correlates with the amount of palladium.

The puzzling question: What causes these explosions Are they inherent to the system or a result of the formation of new entities because .... *there are appropriate thermodynamic conditions for the formation of large clusters of hydrogen nuclei or of regions of the lattice containing ordered arrays of hydrogen nuclei at high H/Pd ratios* [8]. A limited discussion, suggesting that the explosive character is due to a chain reaction, was advanced by Biberian [7]. It is reasonable to assume that a set of events preceded the chain reaction. This assumption appears to be consistent with the data in Fig. 7, sections A B C, and can be further developed if, as the concentration of deuterium increases, the Pd/H–H_2O system transits to the Pd/D–D_2O system. Conditions associated with this transition can be obtained by examining the kinetics of the set of coupled reactions: $e^- + p^+_* \rightarrow n$; $n + p^+_*(\text{or } p^+_l) \rightarrow d^+$; $e^- + d^+ \rightarrow 2n$ This, however, is outside of the scope of this communication.

References

[1] A. Widom and L. Larsen, *Eur. Phys. J.* **C46** (2006) 107–117.

[2] H. Remy, *Treatise on Inorganic Chemistry*, Elsevier, Amsterdam, Vol. II, p. 563, 1956. [*Nuclear reaction may be represented by equations which correspond exactly to those employed in chemical reactions. This section of nuclear physics which deals particularly with transmutation of the elements, occurring in nuclear reactions has appropriately been termed nuclear chemistry.* It goes on to say: *The essential goal of nuclear physics is to interpret the nature of nuclear forces. One important approach to this objective is the study of transmutations occurring in nuclear reactions, and the magnitude of energy liberated in such processes.*]

[3] L.D. Landau and E.M. Lifshitz, *Statistical Phys.*, Vol. 5, Part 1, Pergamon, Oxford, 1957, pp. 318–319. *It is not diffcult to write down the thermodynamic conditions which govern the "one chemical equilibrium" of the nuclear reaction, which may be symbolically written as* $A_Z + e^- \rightarrow A_{Z-1} + \nu$, *where* A_Z *denotes nucleus of atomic weight A and charge Z,* e^- *an electron and* ν *a neutrino. The neutrinos are not retained by matter and leave the body.*

[4] H.W, Washburn, C.E. Berry and H.G. Hall, *Anal. Chem.* **25** (1953)130.

[5] P.A. Mosier-Boss, S. Szpak, F.E. Gordon and L.P.G. Forsley, *Naturwissenschaften* **96** (2008) 135–142.

[6] M. Fleischmann, private communication.

[7] J.-P. Biberian, *J. Condensed Matter Nucl. Sci.* **2** (2009) 1.

[8] M. Fleishmann, S. Pons and G. Peparata, *Il Nuovo Cimento* **107 A** (1994) 143.